Hindawi
Journal of Sensors
Volume 2017, Article ID 9643279, 12 pages
https://doi.org/10.1155/2017/9643279

Research Article

A Model-Based Virtual Sensor for Condition Monitoring of Li-Ion Batteries in Cyber-Physical Vehicle Systems

Luciano Sánchez,[1] Inés Couso,[2] José Otero,[1] Yuviny Echevarría,[1] and David Anseán[3]

[1]*Computer Science Department, Universidad de Oviedo, Oviedo, Spain*
[2]*Statistics Department, Universidad de Oviedo, Oviedo, Spain*
[3]*Electrical Engineering Department, Universidad de Oviedo, Oviedo, Spain*

Correspondence should be addressed to Luciano Sánchez; luciano@uniovi.es

Received 7 March 2017; Accepted 27 August 2017; Published 12 October 2017

Academic Editor: Qing Tan

A model-based virtual sensor for assessing the health of rechargeable batteries for cyber-physical vehicle systems (CPVSs) is presented that can exploit coarse data streamed from on-vehicle sensors of current, voltage, and temperature. First-principle-based models are combined with knowledge acquired from data in a semiphysical arrangement. The dynamic behaviour of the battery is embodied in the parametric definition of a set of differential equations, and fuzzy knowledge bases are embedded as nonlinear blocks in these equations, providing a human understandable reading of the State of Health of the CPVS that can be easily integrated in the fleet through-life management.

1. Introduction

Cyber-physical vehicle systems (CPVSs) integrate locomotion, computational, and communication components, aiming to leverage interdependent behaviour by integrating control, computing, communications, and physical systems [1]. Monitoring, fault detection, and diagnosis of CPVSs are achieved through a combination of hardware sensors and decision-making software [2], often by "anytime" or "imprecise computing" algorithms that balance resources and performance, refining the solutions when the resources become available [3] or degrading gracefully with reduced cyber resources [4]. On the physical side, health monitoring of rechargeable batteries is an important part of both the monitoring and the energy management subsystems of a vehicle and measures the *battery ageing* that can manifest itself either as a gradually decreasing capacity (understood as the amount of electric charge that can be stored and released), a downtrending efficiency when the battery is charged or discharged or, in certain cases, as a catastrophic failure that destroys the cell [5].

Energy management algorithms for CPVS fleets should take into account the fact that the batteries in the vehicles are in different health conditions. Monitoring the battery health in due course has profound practical consequences, because there are silent deteriorations (those that cannot be perceived through a loss of capacity) that can trigger a sudden failure if not detected and acted upon. Ideally, the Battery Management Systems (BMSs) embedded in the powertrains of the vehicles should monitor the State of Health (SoH) of the batteries and notify the supervisor if a degradation is detected. However, as of yet there are no commercially available sensors of the health of a battery that can be used for this purpose. In this paper it is proposed that a virtual sensor (soft sensor) of the SoH is developed that combines signals already present in the BMS and also makes use of a battery model for synthesizing a "health signal" that is sent to the supervisor if an incipient degradation is detected.

Certain "first-principles" (electrochemical) models can estimate health-related variables taking current, voltage, and temperature as inputs [6]. Since these three inputs are available in standard BMSs, these models could, in principle, be part of the proposed virtual sensor. However, electrochemical processes during charge and discharge are different whether the battery is new or aged. Thus, first-principle models are not

effective in mutable scenarios, such as a fleet of CPVSs with different ages.

Learning models (equivalent circuits, statistical methods, neural networks, etc.) could be better suited for the problem being considered. It is remarked that pure data-driven models are not adequate either, because these models may generalize wrongly when subjected to unforeseen combinations of the input variables. For instance, a data-driven model that is learnt with data sampled from charge-discharge cycles at low currents will perform poorly when the current is high. Conversely, a "first-principles" model of a cell that is able to reproduce the behaviour of a new battery for both small and high currents will be inaccurate when applied to an ageing battery, as mentioned. A balance must be sought between the learning capabilities of the model and the amount of prior knowledge about the electrochemical processes that is placed in the model definition. To this we can add that the quality of on-vehicle measurements of current, voltage, and temperature is low, this being particularly true for the temperature. Generally speaking, the uncertainty in the values of the input variables lowers the accuracy of any kind of model, but some models are more resilient to uncertainty than others. Because of these reasons, a computational intelligence-based soft sensor is proposed that is intermediate between first-principle and pure data-driven models, as it is based on a "grey-box" model of the battery. By "grey-box" it is meant that the model is learnt from data, but at the same time it depends on physically meaningful parameters of the battery. The virtual sensor introduced in the present contribution is based on an "imprecise computing" model that exploits unreliable data streamed from on-vehicle sensors of current, voltage, and temperature. Parts of the proposed sensor are implemented with Fuzzy Rule-Based Systems (FRBS) that are fitted to operational data with Genetic Fuzzy Systems (GFSs).

The structure of the paper is as follows: in Section 2, the literature about fast methods for determining the health of a battery is reviewed. In Section 3, the proposed model is introduced. In Section 4, numerical results are provided. The paper concludes in Section 5 with some remarks and a list of yet-unsolved problems and challenges.

2. State of the Art in the State of Health Monitoring

The best reported methods for assessing battery health compute the functional dependence between the stored charge and the open circuit voltage (OCV) of the battery at equilibrium, by determining the positions of the peaks at the Incremental Capacity (ICA) [7]. This last curve is obtained by differentiating the battery charged capacity with respect to the OCV. In Figure 1(a), an example of the evolution in time of the ICA curve is shown, measured at one of the batteries used in this study. Alternatively, the inverse derivative (OCV with respect to the capacity) is the Differential Voltage (DVA) curve that also gives a clear insight of the efficiency of the battery (see Figure 1(b)). In both cases, a precise knowledge of the OCV is crucial for monitoring the condition of automotive batteries.

The most accurate method for obtaining the OCV is the "voltage relaxation" procedure [8]. Voltage relaxation consists in a sequence of short calibrated incremental charges (or discharges) that are combined to obtain a pointwise estimation of the OCV curve. However, this method is extremely slow and therefore unsuitable for on-board monitoring (in this particular case, the battery had to be removed from the vehicle for 4 days). In Figure 1(c), a graph showing voltage and current of a battery during an actual voltage relaxation essay is displayed.

Given that relaxation experiments are not a practical method for determining the OCV curve of the battery of a CPVS, accelerated methods are a must. However, these curves must be determined while the battery is at equilibrium, that is, when a charge (discharge) current is not flowing [9]. In practical circumstances, ICA and DVA analysis can be carried out when a current is flowing that is not higher than 1/25 of the capacity of the battery measured in Ah (or "C25" cycle); thus direct measurements are not reliable if they are completed in less than 25 hours [10].

Different procedures have been published where the OCV is approximated with data sampled during lapses shorter than a day, with varying accuracies; see, for instance, [11–15]. The problem is harder when the time window is shortened: if the battery has to be drained faster, the discharge current has to be raised accordingly and the memory effects of the battery are no longer negligible. Unfortunately, it is difficult to model the memory effects of a Li-Ion battery. As mentioned in Introduction, neither first-principles (or "white boxes") nor data-driven (or "black boxes") methods are valid. On the one hand, although the electrochemical, thermodynamic, and transport phenomena that define the behaviour of a Li-Ion battery are well known [16], white models are not valid because these models depend on a large number of parameters that are not provided by the manufacturer [17]. On the other hand, black boxes are unreliable when predicting unforeseen states and cannot incorporate prior knowledge about the mentioned phenomena [18]. A balance between white and black boxes is needed, and these are the "grey boxes," also known as "semiphysical models."

Grey models are a compromise where some parts of the definition of the model are taken from granted and other parts are learnt from data. The most prevalent grey boxes are equivalent circuit models, where the battery is assimilated to an electrical circuit comprising a network of resistances and capacitors [19]. SoH observers have been derived from equivalent circuit models; see, for instance, [20, 21]. These models produce estimations of the OCV whose accuracy is good (about ±1%) for a range of State of Charge (SoC) between 20 and 90%, provided that the charge/discharge current is between low and moderate. Since these equivalent circuit models are not based on electrochemical properties of the battery, the parameters of the OCV curve cannot be directly deduced from the values of the capacitors and resistances in the network. However, these models can be subjected to virtual experiments in accelerated time; that is, a relaxation experiment that lasts more than one day with real-world batteries can be simulated with the battery model in milliseconds. The "pseudo-OCV" curves that are

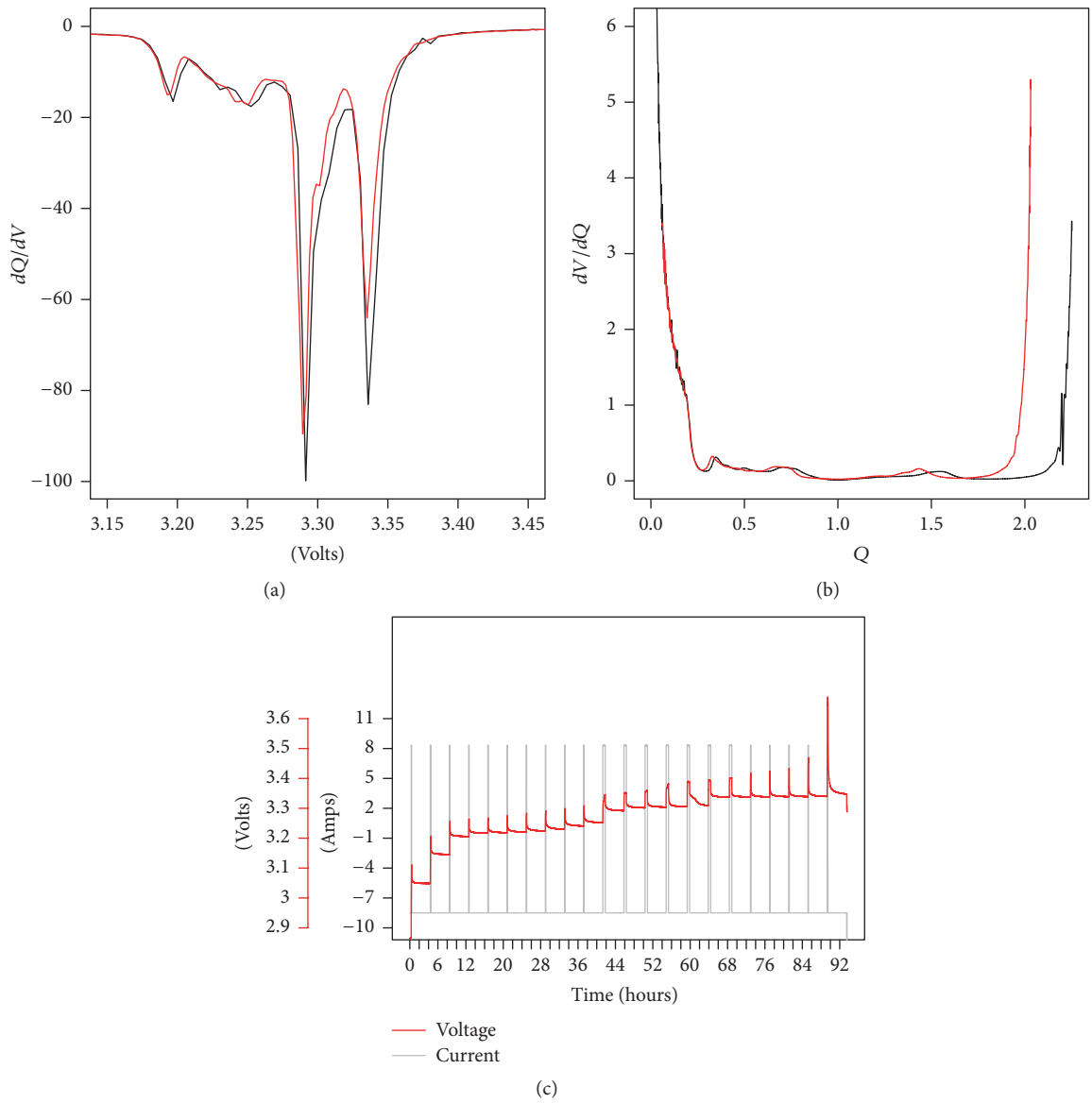

Figure 1: ICA (a) and DVA (b) curves of a new $LiFePO_4$ battery are drawn in black. These curves are superimposed in red for the same battery after 3000 charge-discharge cycles. The diagnostic of the battery is immediate when these curves are available. (c) Current and voltage during the experimental OCV determination by voltage relaxation of a typical $LiFePO_4$ battery. The relaxation time between partial charges is on 4 h. Pulses are of 10% of the battery capacity (42 Ah). OCV, IVA, and DVA can be measured at the laboratory, but the procedure is long, lasting more than four days in batteries with higher capacities. A soft sensor is sought that produces these curves through data sampled with on-vehicle sensors.

obtained from virtual experiments could, in principle, be processed to recover ICA or DVA graphs (see, e.g., [7]) but the accuracy of this kind of "virtual laboratory" experiments is poor.

3. A Semiphysical Model-Based Soft Sensor of the SoH

Other kinds of grey boxes have been successfully used in State of Charge (SoC) predictive models [22, 23], and these can be adapted to the problem at hand with certain modifications. These models are based on a physical analogy between charging a battery and filling a flexible vessel, because the function linking the height of a fluid with its mass, in a vessel with the appropriate shape, can also measure the interdependence between the voltage of a battery and its charge.

In this section, a design of an ensemble of Fuzzy Rule-Based Systems (FRBS) and differential equations is presented. The design follows the principles stated in [24] and is aimed to obtain an estimation of the SoH: after this ensemble is fitted to data, the KB of one of its member FRBS comprises a set of "if-then" rules describing the SoH of the battery through its OCV. This new definition allows that the SoH is inferred from the learnt parameters of the model without the need of a "virtual lab" relaxation experiment.

3.1. Notation. The on-vehicle signals are the charge current, $I(t)$, the battery voltage, $V(t)$, the battery temperature, $T(t)$, and the ambient temperature, $T_{\text{amb}}(t)$. The hidden variables are the electrical charge $\text{SoC}(t)$ and the overpotential $\text{OP}(t)$, which is the difference between the voltage of the battery and the OCV for the same SoC. The outputs of the soft sensor comprise the OCV curve of the battery (as a function of the SoC), $V(t)$, $T(t)$, and the hidden variables $\text{OP}(t)$ and $\text{SoC}(t)$, given the inputs $I(t)$, $T_{\text{amb}}(t)$ and the initial charge of the battery $\text{SoC}(0)$.

3.2. Battery Modelling with Fuzzy Rule-Based Systems. Batteries are complex systems. A black-box model is possible but it would require a long time window and training data covering many different scenarios, which is not always available (or attainable). However, the electrochemical processes that happen when batteries are charged are well known; thus there is a high potential for injecting expert knowledge into the model (by means of if-then rules, physical analogies, etc.) This addition of knowledge is intended to avoid that the algorithm that learns the model from data ends up confirming what is already known.

There are many different contributions regarding the balance between accuracy and interpretability in FRBS [25]. Most of these studies are intended to improve the linguistic interpretability of models that are intended for verbal communication (i.e., for explaining the model properties to a human expert). The proposed model conveys the reverse path, that is, injecting human knowledge; thus the model generalizes well for situations not present in the training data.

In this particular case, there are certain pieces of knowledge about the dynamic behaviour of the battery that can be efficiently represented by means of differential equations. An outline of the sensor structure is illustrated in Figure 2. The sensor comprises a combination of dynamical blocks including three FRBSs, representing the following.

(1) OCV versus SoC. This is the main output of the proposed soft sensor. The only input to this system is the SoC, which is the cumulative sum of the charge current, discounting the charging losses. There is a dotted input in the diagram, indicating that the OCV should also depend on the battery temperature, but this dependence can be safely ignored for LiFePO_4 batteries [26]. The output of this FRBS is the voltage of the battery at equilibrium.

(2) Overpotential in Steady State versus SoC and Temperature. This FRBS models the difference between the output voltage and the OCV when the battery is being charged (or discharged) at a constant pace. The inputs to this second system are the SoC and the battery temperature. Its output is not routed to the exterior but is fed to a feedback loop along with the net charging current that models the kinetic behaviour of the battery. The output of this feedback loop is added to the OCV to produce the second output of the sensor, the predicted battery voltage. The difference between the prediction of the battery voltage and the measured voltage is the first of the error signals which will be minimized during the learning process.

(3) Internal Calorific Power versus SoC and Current. The third FRBS models the heat emission of the battery as a function of the SoC and the charging current. The output of this system is not routed to the exterior either, but it is the input of an internal dynamical model of the temperature of the battery that depends on the specific heat of the cell and the thermal resistance between the cooling system and the ambient. The difference between the output of the dynamical model of the battery and the ambient temperature is the second error signal, which is also minimized during the learning.

3.3. Equations of the Sensor. The equations associated with the model in Figure 2 are detailed in this section. These equations encode the expert knowledge about the battery behaviour through the parametric definition of a set of differential equations. The available expertise about the battery dynamics is summarized in the following list.

(1) Nonreversible Energy Losses Are Proportional to the Charging Current, by a Factor That Depends on the Charge. Charging or discharging the battery is not a completely efficient process. There are energy losses and, to a lesser degree, charging losses that are handled by multiplying the input current by a factor (about 0.999 in this study; this is the "charging losses" box). Energy losses are modelled by a parasitic series voltage PV, proportional to the current ("power losses" box):

$$\text{Energy losses} = \left| I \cdot \text{PV}\left(\text{SoC}, I\right)\right|. \tag{1}$$

The absolute value is needed because the current is negative when discharging. In this model the simplification $\text{PV}(\text{SoC}, I) \approx k \cdot I$ is made, for a constant k that is learnt from data; thus the nonreversible energy losses are proportional to the square of the current.

(2) The Difference between the Voltage at Equilibrium and the Voltage While Charging (or Discharging) Depends on Charge, Current, and Temperature. The output voltage will be modelled as the sum of three terms: (a) the voltage in equilibrium, OCV, that depends on charge and temperature (this dependence is modelled by FRBS 1 in Figure 2), although in the particular case of LiFePO_4 technology the dependence between OCV and temperature was disregarded, as mentioned; (b) the overpotential, OP, that depends on charge, current, and temperature (FRBS 2 and diffusion process, in the same figure); (c) parasitic voltage associated with energy losses ("power losses" box)

$$V\left(\text{SoC}, T, I\right) = \text{FRBS}_1\left(\text{SoC}\right) + \text{OP}\left(\text{SoC}, T, I\right) + k \cdot I. \tag{2}$$

(3) The Voltage of the Battery in Open Circuit Keeps Changing for a Certain Time after a Charge or a Discharge Is Applied (Voltage Relaxation). Charging or discharging the battery involves diffusion processes, whose speed is limited: it is not physically possible to charge a battery in a very short time. According to our experimentation, a first-order differential equation or exponential decay with time constant τ is enough to acknowledge this constraint:

$$\tau \cdot \dot{\text{OP}} = -\text{OP} + I \cdot \text{FRBS}_2\left(\text{SoC}, T, \text{sign}\left(I\right)\right). \tag{3}$$

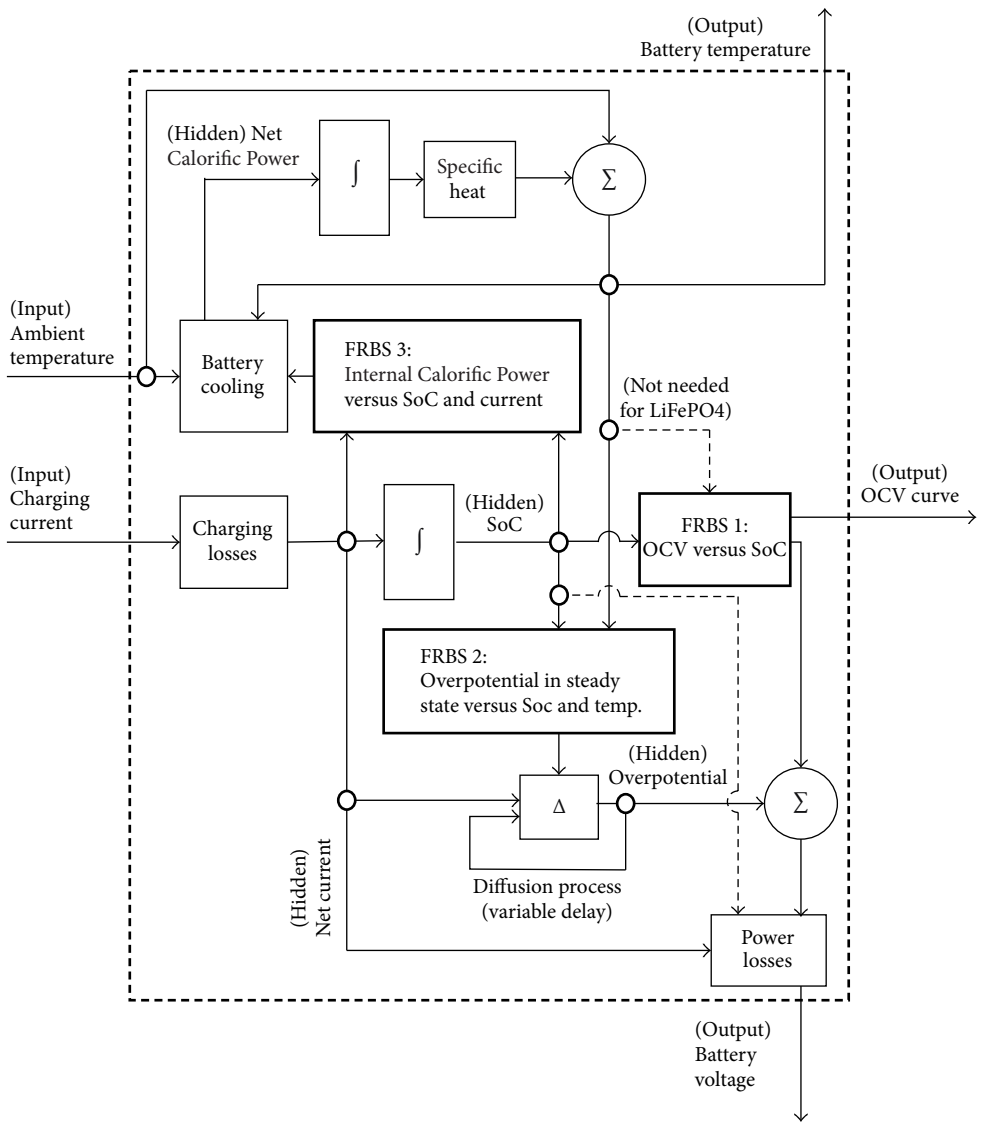

Figure 2: Block-based representation of the proposed soft sensor. OCV, overpotential, and Calorific Power are represented by FRBSs. These FRBSs can only be learnt from data in an indirect manner, by comparing the simulations of the model with the evolution of the observable variables and tuning the fuzzy rules in the three FRBSs until these trajectories become identical.

The forcing function is $I \cdot \mathrm{FRBS}_2(\mathrm{SoC}, T, \mathrm{sign}(I))$, where FRBS_2 can be understood as a charge-dependant impedance that models the linearized quotient between overpotential and current. If the current is 0, OP eventually also becomes 0, modelling the voltage relaxation mentioned before. Small batteries have low τ, that is, quick dynamics and vice versa.

(4) The Temperature of the Battery Depends on the Integral of the Difference between Generated and Dissipated Calorific Power. It is proposed that the dynamic properties of the battery temperature are approximated by this equation:

$$c \cdot \dot{T} = -\rho\left(T - T_{\mathrm{amb}}\right) + |I \cdot \mathrm{OP}| + I^2\left[k + T \cdot \mathrm{FRBS}_3\left(\mathrm{SoC}, \mathrm{sign}\left(I\right)\right)\right], \tag{4}$$

where c is the specific heat of the battery and ρ is the thermal conductance with the ambient. The term $I^2 k$ was explained in (1). The thermal power resulting from entropy changes, that is, $\partial(\mathrm{OCV})/\partial T$ in accordance with Helmholtz equation [27], is modelled by the triple product of (a) the output of FRBS_3; (b) the absolute temperature of the battery; and (c) the square of the current. It is remarked that the output of FRBS_3 may be negative, when the battery absorbs heat in a reversible process.

Summarizing, the differential equations describing the dynamics of the sensor model are

$$\dot{\mathrm{SoC}} = I$$

$$V = \mathrm{FRBS}_1 + \mathrm{OP} + k \cdot I$$

$$\tau \cdot \dot{\mathrm{OP}} = -\mathrm{OP} + I \cdot \mathrm{FRBS}_2$$

$$c \cdot \dot{T} = -\rho\left(T - T_{\text{amb}}\right) + |I \cdot \text{OP}| + I^2\left[k + T \cdot \text{FRBS}_3\right], \tag{5}$$

where $\text{FRBS}_1(\text{SoC})$, $\text{FRBS}_2(\text{SoC}, T, \text{sign}(I))$, and $\text{FRBS}_3(\text{SoC}, \text{sign}(I))$ are rule-based systems that are indirectly learnt from operation data, as described in the following subsection.

3.4. Learning Algorithm. Assuming that the battery temperature is controlled (thus there are no extreme temperature changes during the operation of the vehicle), the sensor equations can be discretized through the implicit Euler's method [28]:

$$\begin{aligned}
&\text{SoC}_{t+1} = \text{SoC}_t + \Delta t \cdot I_{t+1} \\
&\text{OP}_{t+1} = \frac{1}{\tau + \Delta t}\left[\tau \cdot \text{OP}_t + \Delta t \cdot I_{t+1}\right. \\
&\quad \left. \cdot\, \text{FRBS}_2\left(\text{SoC}_{t+1}, \text{sign}\left(I_{t+1}\right)\right)\right] \\
&V_{t+1} = \text{FRBS}_1\left(\text{SoC}_{t+1}\right) + \text{OP}_{t+1} + k \cdot I_{t+1} \\
&T_{t+1} \\
&\quad = \frac{\Delta t \cdot \left[\rho \cdot T_{\text{amb},t+1} + \left|I_{t+1} \cdot \text{OP}_{t+1}\right| + I_{t+1}^2 \cdot k\right] + c \cdot T_t}{c + \Delta t \cdot \left(\rho + I_{t+1}^2 \cdot \text{FRBS}_3\left(\text{SoC}_{t+1}, \text{sign}\left(I_{t+1}\right)\right)\right)},
\end{aligned} \tag{6}$$

where SoC_t stands for $\text{SoC}(t)$, SoC_{t+1} means $\text{SoC}(t + \Delta t)$, and so forth.

Assuming that SoC_0 is known and given a sequence of N samples of the input variables, I_t and $T_{\text{amb},t}$ for $t = 1, 2 \ldots, N$, then the computer simulation of the outputs V_t and T_t and the hidden variables OP_t and SoC_t consists in successive applications of (6), once for each time period t.

Given a sequence of on-vehicle sampled values V_t^*, T_t^* and the initial charge SoC_0^*, learning this model from data consists in determining

(1) the constants k, τ, ρ, and c,

(2) the rule-based systems $\text{FRBS}_1(\text{SoC})$, $\text{FRBS}_2(\text{SoC}, T, \text{sign}(I))$, and $\text{FRBS}_3(\text{SoC}, \text{sign}(I))$

that minimize the dissimilarities between the computer simulation and the measured values.

As mentioned, on-vehicle measurements are not reliable and nonlinear least squares are not robust in these conditions, because a single outlier can alter the results. The rule learning algorithm described in [29] is resilient to the presence of outliers and will be used here. This algorithm is based on the genetic optimization of a multivariate fuzzy-valued error which is a function of the parameters described before. This fuzzy function is described in the following paragraphs.

Let us suppose that the difference between the true temperature of the battery T_t^{true} and the perceived temperature T_t^{perc} is lower than a certain bound δ_α^T with a probability greater than $1 - \alpha$,

$$\begin{aligned}
\mathbf{T}_t^\alpha &= \left[T_t^{\text{perc}} - \delta_\alpha^T, T_t^{\text{perc}} + \delta_\alpha^T\right] \\
P\left(T_t^{\text{true}} \in \mathbf{T}_t^\alpha\right) &\geq 1 - \alpha.
\end{aligned} \tag{7}$$

Observe that the most specific estimation of the squared error of the model for each level α is

$$\text{err}_T^\alpha = \left\{\sum_{T=1}^{N}\left(T_t - \tau_t\right)^2 : \tau_t \in \mathbf{T}_t^\alpha\right\} \tag{8}$$

and the same course of reasoning can be applied to the voltage, for a different set of bounds δ_α^V:

$$\begin{aligned}
\mathbf{V}_t^\alpha &= \left[V_t^{\text{perc}} - \delta_\alpha^V, V_t^{\text{perc}} + \delta_\alpha^V\right] \\
\text{err}_V^\alpha &= \left\{\sum_{t=1}^{N}\left(V_t - \nu_t\right)^2 : \nu_t \in \mathbf{V}_t^\alpha\right\}.
\end{aligned} \tag{9}$$

Following [30], the nested families of sets err_T^α and err_V^α can be regarded as fuzzy sets $\widetilde{\text{err}}_T$ and $\widetilde{\text{err}}_V$, whose membership function is as follows:

$$\begin{aligned}
\widetilde{\text{err}}_T(\tau) &= \sup\left\{\alpha : \tau \in \text{err}_T^\alpha\right\} \\
\widetilde{\text{err}}_V(\nu) &= \sup\left\{\alpha : \nu \in \text{err}_V^\alpha\right\}
\end{aligned} \tag{10}$$

allowing the application of the genetic algorithm described in [29]. It is remarked that values δ_α^V and δ_α^T are tolerance intervals describing the accuracy of on-board sensors. If $\delta_\alpha^V = 0$ and $\delta_\alpha^T = 0$, the procedure described in this section reduces itself to ordinary nonlinear least squares; thus the estimation becomes precise if accurate sensors are available and degrades gracefully when quality information is not available.

4. Numerical Results

The experimental setup, comprising the battery type, the test equipment, and the charging and discharging protocols, is described in the first place. The numerical results of the experimentation are detailed in Section 4.2, including the compared results of the proposed method against a selection of fast OCV estimators.

4.1. Experimental Setup. The tested cell is a LiFePO_4 (LFP) pouch battery from European Batteries (see Figure 3). This cell uses a LFP cathode in combination with graphite anode active material. The rated capacity is 42 Ah at C/5 (the discharge current at C/5 is $42/5 = 8.4$ A). The average operating voltage is 3.2 V. The discharge and charge cut-off voltages are 2.5 V and 3.65 V, respectively. The dimensions in mm are $275 \times 166.5 \times 13.3$. The weight cell is 1010 g.

All tests have been done using a setup that consists of a SBT 10050 battery test system from PEC in combination with an ICP 750 climate chamber from Memmert. All tests were carried out at an ambient temperature of 23°C. Testing-machine adjustments were performed to improve the reliability and accuracy of the measurements. The first stage of the testing procedure was commissioning, during which the battery was identified and weighed. Then, a conditioning test was performed according to the USABC [8]. It consisted of three different constant current (C/3, C/2, and C) discharge cycles. The standard charging method

(a) (b)

Figure 3: (a) SBT 10050 battery test system from PEC and ICP 750 climate chamber. (b) Detail of the $LiFePO_4$ (LFP) pouch battery from European Batteries, rated at 42 Ah at C/5, used in the tests.

provided by the manufacturer was used to charge the cell. This consists of a constant current (CC) stage at C/2 until the cell reaches the charging cut-off voltage, followed by a constant voltage (CV) stage until the current decreases to 0.05 C. For subsequent testing, the battery capacity is considered stable when three successive C3/3 discharges agree within 2%.

After the capacity had stabilized, a full charge/discharge cycle was performed at a rate of C/25. The results of the C/25 measurements provide a practical capacity reference with minimal kinetic effects which is close to the maximum capacity attainable by the cell. The battery capacity was measured at C/5 and the result was 44.6 Ah instead of the rated capacity of 42 Ah. The measured capacity was taken into account for the open circuit voltage (OCV) at equilibrium measurements. To determine the battery OCV the voltage relaxation method was used [20]. With this method the battery voltage relaxes to the OCV at equilibrium after current interruption. To obtain the OCV at equilibrium at different states of charge (SoC) the voltage relaxation measurements were performed by charging and discharging a cell in 4460 mAh steps (approximately 10% of the measured capacity at C/5) at C/5 constant current. At the end of charge/discharge voltage, a constant voltage (CV) stage is applied until $I < C/100$ to ensure full charge/discharge voltage of the cell. Each charge and discharge step was followed by a rest period of 4 hours, after which the voltage was sampled. This voltage was assumed to be equal to the OCV at equilibrium.

Finally, the battery was subjected to discharges at C/5, C/3, C/2, and C constant currents. Discharging was carried out at CC until reaching the discharging cut-off voltage recommended by the manufacturer. There was an inactivity period of one hour after each charge or discharge until the battery temperature fell below 24.5°C.

4.2. Numerical Results and Discussion. In Figure 4 the OCV estimation produced by the proposed method is plotted in blue over the OCV points obtained with the relaxation method (in red). The hysteresis of the charge/discharge cycle used to determine the OCV is plotted along the data.

The slowest cycle at C/25 (50 hours) produced the most accurate estimation, which is in the same error range compared to the relaxation method for charges of 4 Ah and higher (SoC ≥ 10%). The accuracy of the estimation is reduced for C/5, C/3, C/2, and C, but the results are in the 20 mV range for charges as fast as C/2 (4 hours). Observe the excellent results when extrapolating the OCV to 45 Ah from all cycles faster than C/25. The determination of the OCV is not accurate for charges lower than 4 Ah (10% SoC); however this is a problem shared by all fast OCV estimators, as shown later.

The differences in accuracy as a function of the charge/discharge current are shown in detail in Figure 5. Observe that the relaxation method, being the most accurate experimental procedure itself, is also subjected to a small variance of ±10 mV, depending on whether the point was sampled when the cell is being charged or discharged. This variability has been displayed with the red error bars in Figure 5. In addition to this, the mean accuracy of the estimation is plotted against the experimental time in Figure 6, showing that the expected error grows quickly if the current is higher than C/2. The dotted superimposed grey curve is an exponential fitting to the data.

In Table 1 the compared error values (average of the absolute error in volts) of the proposed method and Xu et al.'s [21] and AbuSharkh and and Doerffel's [20] methods are displayed. Points of the relaxation OCV taken at charges higher than 40 Ah were discarded for the C/3, C/2, and C curves. A Friedman test was used to check that there are statistical differences between the methods. Observe that the proposed method was the best in all cases, with a single tie at C/25 between the proposed method and Xu et al.'s. Pairwise Mann–Whitney tests were also applied between the proposed method and each of the alternatives. The differences were regarded as significant when the p value of the Mann–Whitney test is lower than 0.05. Best results were marked in boldface.

To clearly perceive the differences between the proposed algorithm and the best alternative, the OCV estimation with the Xu et al.'s method is shown in Figure 7. Observe that the fitting is less accurate for charges below 8 Ah (20% SoC) or over 40 Ah (89% SoC), and the extrapolation to charges over the sampled data is not as regular as the soft sensor. The differences are clearer in Figure 8, showing that the alternatives are more efficient for small currents (the C/25 curve is not statistically different than the best) and the

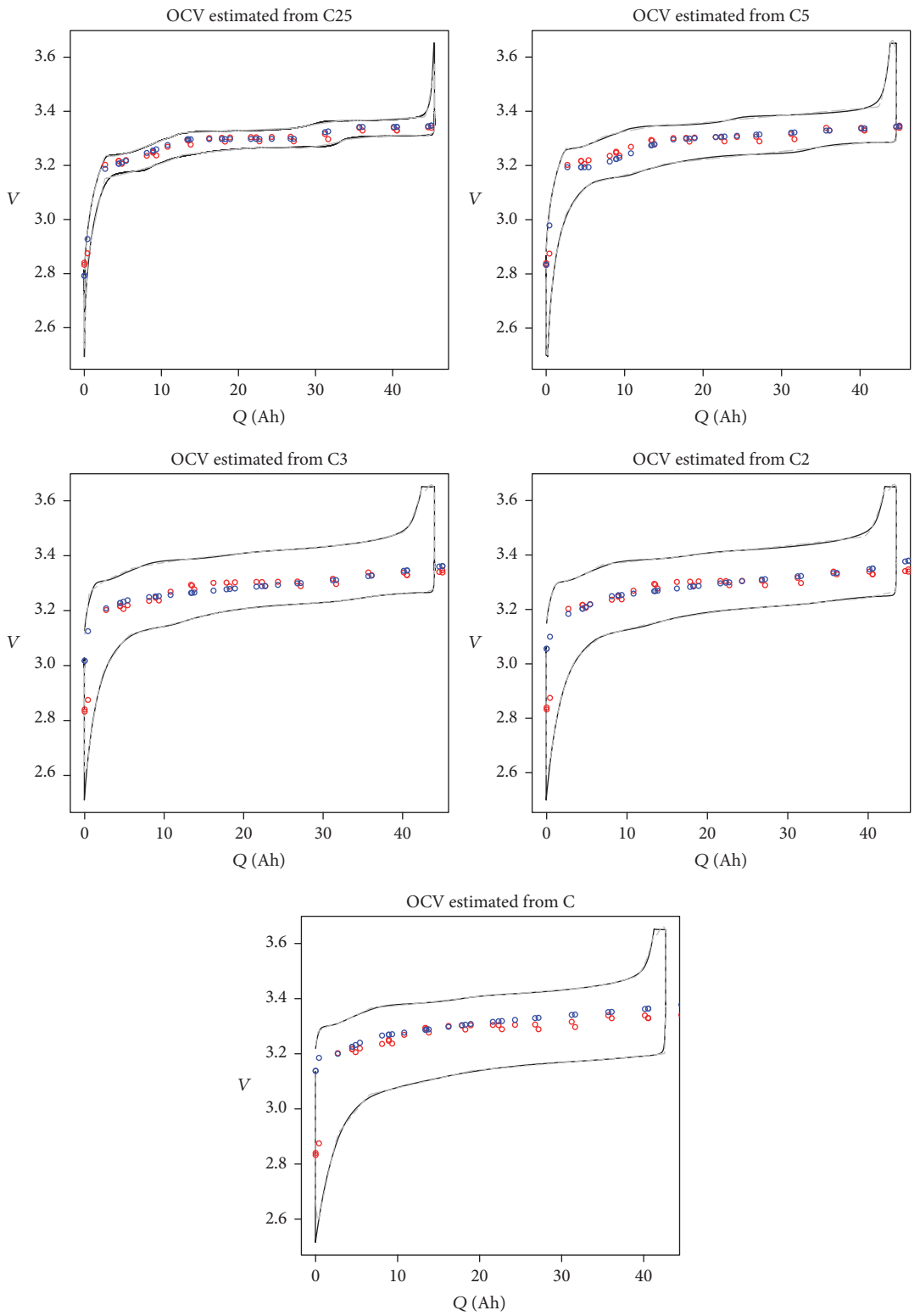

Figure 4: OCV estimated through the proposed method (in blue) over the OCV points obtained with the relaxation method (in red). The charge/discharge cycle used to learn the OCV is plotted along the data.

Table 1: Compared error values (average of the absolute error in volts) of the proposed method and Xu et al.'s [21] and AbuSharkh and Doerffel's [20] methods. The proposed method was the best in all cases, with statistically significant differences (p value of a Mann–Whitney test lower than 0.05). The only nonstatistical difference was at C/25 between the proposed method and Xu et al.'s.

Current	Proposed method	Upper limit (Ah)	Xu et al.'s method [21]	p value	AbuSharkh and Doerffel's method [20]	p value
C/25	**0.0094**	44	**0.0378**	0.1557	0.0393	0.0454
C/5	**0.0117**	44	0.0181	0.0046	0.0192	0.0007
C/3	**0.0117**	40	0.0181	0.0001	0.0192	$1e-05$
C/2	**0.0115**	40	0.0188	$1e-05$	0.0173	$6e-05$
C	**0.0186**	40	0.0188	$1e-05$	0.0188	$1e-05$

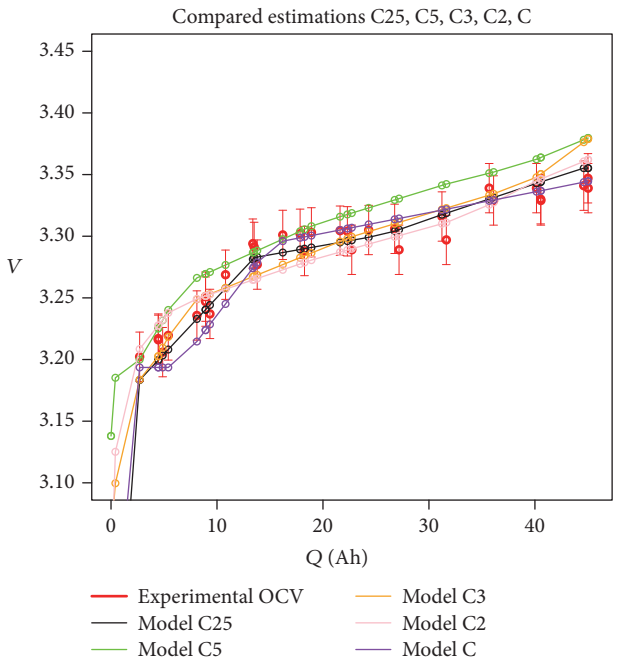

Figure 5: Compared results of the proposed method for charge currents of C/25, C/5, C/3, C/2, and C. The reference points obtained with the relaxation technique are plotted with red error bars.

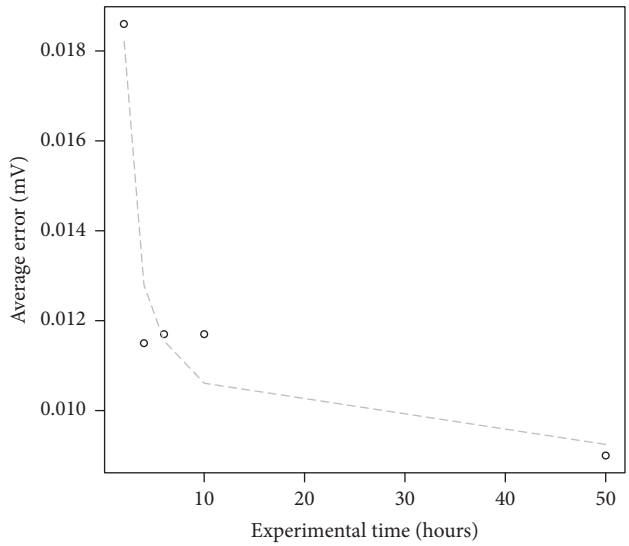

Figure 6: Mean accuracy of the estimation plotted against the experimental time. The expected error grows abruptly if the current is higher than C/2. The dotted grey curve is an exponential fitting to the data.

estimated OCV is not accurate for very low or very high charges, confirming the conclusions expressed by the authors of that method.

5. Concluding Remarks and Future Work

A novel model-based soft sensor for fault detection and diagnosis of rechargeable batteries for CPVSs has been proposed. The main contribution of the present work is the implementation of an "imprecise computing," learning semi-physical model of a battery. The proposed model contains three learnable FRBSs, connected with different dynamical blocks, in a setup that allows obtaining certain parameters of the underlying physical process that are costly or hard to estimate with a dedicated experiment. In particular, this virtual sensor is able to approximate the SoH of an automotive battery from on-vehicle measurements of current, voltage, and temperature, being resilient to inaccurate sensors. The present approximation is much faster than direct measurements by relaxation and the range of application of the new method extends that of the alternatives to SoCs under 20% and over 80%.

The results are promising but there is still a margin for improvement. The dependence between the time constants of the model, the current, and the charge is prone to overfitting, and it is possible that a new set of differential equations would exist that allows for a better fitting for SoCs below 10%. In future works, the first-order assumption for the dynamics of the overpotential will be dropped and replaced by a fractional-order differential equations model. Also, it is remarked that the experiments have been made in an off-vehicle temperature controlled environment. Further experiments are needed where the battery temperature is subjected to larger changes for different use patterns.

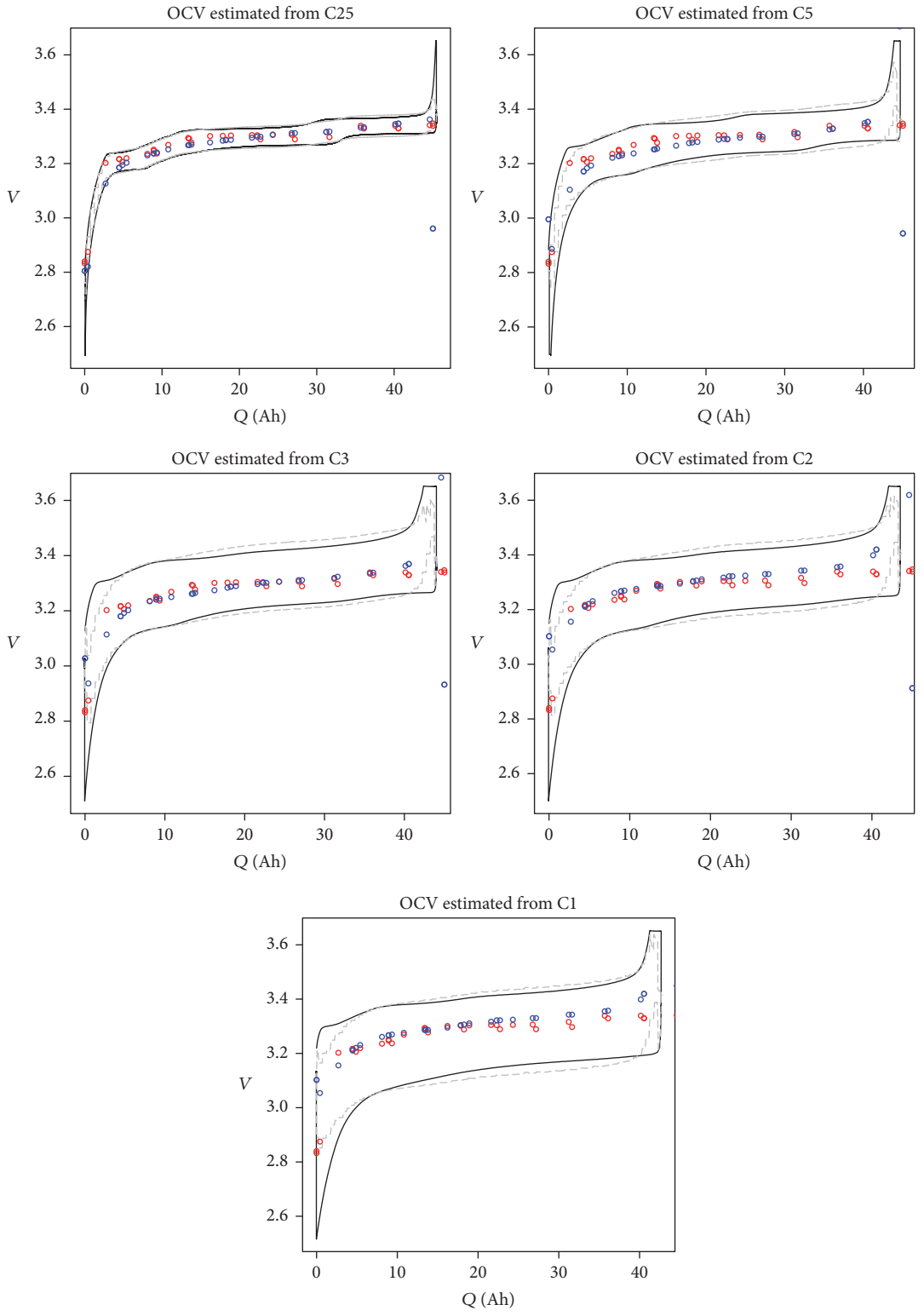

Figure 7: OCV estimated through Xu et al.'s method (in blue) over the OCV points obtained with the relaxation method (in red). The charge/discharge cycle used to learn the OCV is plotted along the data. Observe that the fitting is inaccurate for charges below 8 Ah (20% SoC) or over 40 Ah (89% SoC).

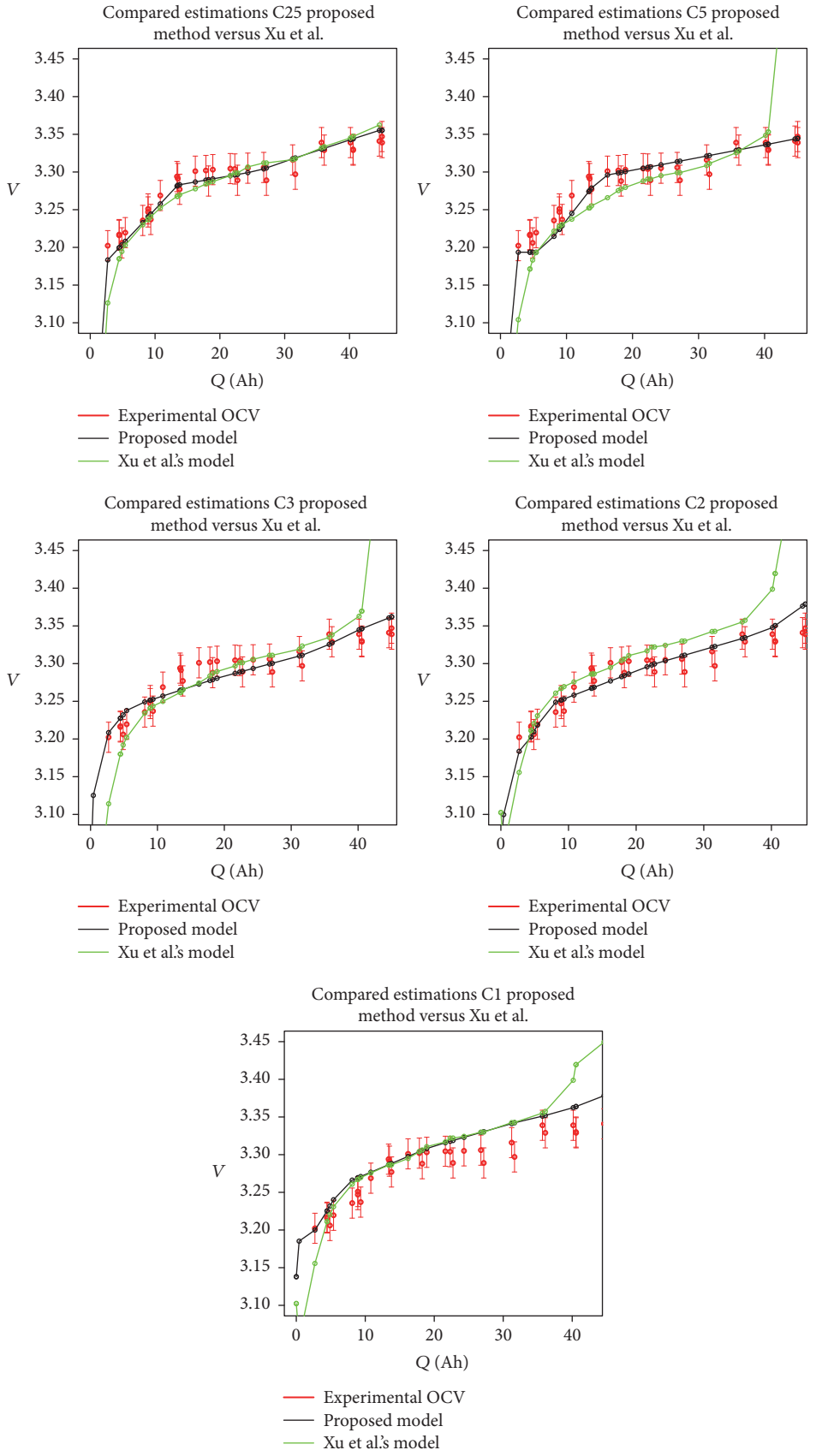

Figure 8: OCV estimations with a semiphysical fuzzy model and Xu et al.'s method. The fitting is less accurate for charges below 8 Ah (20% SoC) or over 40 Ah (89% SoC), and the extrapolation to charges over the sampled data is not as regular as semiphysical model.

Conflicts of Interest

The authors declare that they have no conflicts of interest.

Acknowledgments

This work was supported in part by the Spanish Ministry of Science and Innovation (MICINN) and the Regional Ministry of the Principality of Asturias under Grants TIN2014-56967-R, TIN2017-84804-R, DPI2013-46541-R, and FC-15-GRUPIN14-073, in addition to the Eureka SD Project (Agreement no. 2013-2591) that is supported by the Erasmus Mundus Programme of the European Union.

References

[1] J. M. Bradley and E. M. Atkins, "Optimization and control of cyber-physical vehicle systems," *Sensors*, vol. 15, no. 9, pp. 23020–23049, 2015.

[2] N. Srivastava and J. Srivastava, "A hybrid-logic approach towards fault detection in complex cyber-physical systems," in *Proceedings of the Annual Conference of the Prognostics and Health Management Society*, vol. 1316, Portland, Oreg, USA, 2010.

[3] D. E. Quevedo and V. Gupta, "Sequence-based anytime control," *IEEE Transactions on Automatic Control*, vol. 58, no. 2, pp. 377–390, 2013.

[4] S. J. Russell and S. Zilberstein, "Composing real-time systems," in *Proceedings of the 12th International Joint Conference on Artificial Intelligence (IJCAI '91)*, vol. 91, pp. 212–217, 1991.

[5] J. Vetter, P. Novák, M. R. Wagner et al., "Ageing mechanisms in lithium-ion batteries," *Journal of Power Sources*, vol. 147, no. 1-2, pp. 269–281, 2005.

[6] A. Barré, B. Deguilhem, S. Grolleau, M. Gérard, F. Suard, and D. Riu, "A review on lithium-ion battery ageing mechanisms and estimations for automotive applications," *Journal of Power Sources*, vol. 241, pp. 680–689, 2013.

[7] C. Weng, J. Sun, and H. Peng, "A unified open-circuit-voltage model of lithium-ion batteries for state-of-charge estimation and state-of-health monitoring," *Journal of Power Sources*, vol. 258, pp. 228–237, 2014.

[8] U.S.A.B. Consortium, "Electric vehicle battery test procedures manual," Tech. Rep., 1996.

[9] T. Reddy and D. Linden, *Linden's Handbook of Batteries*, McGraw-Hill, New York, NY, USA, 4th edition, 2010.

[10] D. Ansean, M. Gonzalez, V. Garcia, J. Viera, J. C. A. Anton, and C. Blanco-Viejo, "Evaluation of $LiFePO_4$ batteries for electric vehicle applications," *IEEE Transactions on Industry Applications*, vol. 51, no. 2, pp. 1855–1863, 2015.

[11] I. Snihir, W. Rey, E. Verbitskiy, A. Belfadhel-Ayeb, and P. H. L. Notten, "Battery open-circuit voltage estimation by a method of statistical analysis," *Journal of Power Sources*, vol. 159, no. 2, pp. 1484–1487, 2006.

[12] S. Tong, M. P. Klein, and J. W. Park, "On-line optimization of battery open circuit voltage for improved state-of-charge and state-of-health estimation," *Journal of Power Sources*, vol. 293, pp. 416–428, 2015.

[13] M. A. Roscher and D. U. Sauer, "Dynamic electric behavior and open-circuit-voltage modeling of $LiFePO_4$-based lithium ion secondary batteries," *Journal of Power Sources*, vol. 196, no. 1, pp. 331–336, 2011.

[14] T. Stockley, K. Thanapalan, M. Bowkett, and J. Williams, "Design and implementation of OCV prediction mechanism for PV-lithium ion battery system," in *Proceedings of the 20th International Conference on Automation & Computing (ICAC '14)*, pp. 49–54, September 2014.

[15] B. Xiao, Y. Shi, and L. He, "A universal state-of-charge algorithm for batteries," in *Proceedings of the 47th Design Automation Conference (DAC '10)*, p. 687, ACM Press, Anaheim, Calif, USA, June 2010.

[16] M. Yoshio, R. J. Brodd, and A. Kozawa, *Lithium-Ion Batteries*, Springer, New York, NY, USA, 2009.

[17] A. Seaman, T.-S. Dao, and J. McPhee, "A survey of mathematics-based equivalent-circuit and electrochemical battery models for hybrid and electric vehicle simulation," *Journal of Power Sources*, vol. 256, pp. 410–423, 2014.

[18] Y. Oussar and G. Dreyfus, "How to be a gray box: Dynamic semi-physical modeling," *Neural Networks*, vol. 14, no. 9, pp. 1161–1172, 2001.

[19] U. Westerhoff, K. Kurbach, F. Lienesch, and M. Kurrat, "Analysis of lithium-ion battery models based on electrochemical impedance spectroscopy," *Energy Technology*, vol. 4, no. 12, pp. 1620–1630, 2016.

[20] S. AbuSharkh and D. Doerffel, "Rapid test and non-linear model characterisation of solid-state lithium-ion batteries," *Journal of Power Sources*, vol. 130, no. 1-2, pp. 266–274, 2004.

[21] J. Xu, B. Cao, Z. Chen, and Z. Zou, "An online state of charge estimation method with reduced prior battery testing information," *International Journal of Electrical Power and Energy Systems*, vol. 63, pp. 178–184, 2014.

[22] C. Blanco, L. Sanchez, M. Gonzalez, J. C. Anton, V. Garcia, and J. C. Viera, "An equivalent circuit model with variable effective capacity for $LiFePO_4$ batteries," *IEEE Transactions on Vehicular Technology*, vol. 63, no. 8, pp. 3592–3599, 2014.

[23] L. Sanchez, C. Blanco, J. C. Anton, V. Garcia, M. Gonzalez, and J. C. Viera, "A variable effective capacity model for $LiFePO_4$ traction batteries using computational intelligence techniques," *IEEE Transactions on Industrial Electronics*, vol. 62, no. 1, pp. 555–563, 2015.

[24] L. Sánchez, I. Couso, and M. González, "A design methodology for semi-physical fuzzy models applied to the dynamic characterization of $LiFePO_4$ batteries," *Applied Soft Computing*, vol. 14, pp. 269–288, 2014.

[25] J. Casillas, O. Cordón, F. H. Triguero, and L. Magdalena, *Interpretability Issues in Fuzzy Modeling*, vol. 128, Springer, 2013.

[26] J. Li, J. Klee Barillas, C. Guenther, and M. A. Danzer, "A comparative study of state of charge estimation algorithms for $LiFePO_4$ batteries used in electric vehicles," *Journal of Power Sources*, vol. 230, pp. 244–250, 2013.

[27] M. Hazewinkel, *Encyclopaedia of Mathematics: "Helmholtz Equation"*, Springer Science & Business Media, 2013.

[28] J. C. Butcher, *Numerical Methods for Ordinary Differential Equations*, John Wiley & Sons, 2003.

[29] L. Sánchez, I. Couso, and J. Casillas, "Genetic learning of fuzzy rules based on low quality data," *Fuzzy Sets and Systems*, vol. 160, no. 17, pp. 2524–2552, 2009.

[30] I. Couso and L. Sánchez, "Higher order models for fuzzy random variables," *Fuzzy Sets and Systems*, vol. 159, no. 3, pp. 237–258, 2008.